

DOI: 10.1002/ange.200502847

Compounds with the “Maple Leaf” Lattice: Synthesis, Structure, and Magnetism of $M_x[Fe(O_2CCH_2)_2NCH_2PO_3]_6 \cdot nH_2O^{**}$

Dale Cave, Fiona C. Coomer, Eduardo Molinos, Hans-Henning Klauss, and Paul T. Wood*

Compounds in which geometric frustration is present in an extended lattice are attracting a great deal of attention,^[1] because the degeneracy of the spin ground state in such materials can lead to exotic magnetic behavior, such as the formation of spin liquid^[2,3] and spin ice^[4,5] phases. To prepare new frustrated lattices, methods must be developed to construct materials based on odd-sided polygons with anti-ferromagnetic coupling. Since anti-ferromagnetic exchange interactions are common, the second requirement is easily fulfilled. As the triangle is the only odd-sided polygon which can be packed into an extended array, this is the only building block we need to consider. Possible triangular bridges include TO_4^{n-} ions such as phosphate, sulfate, or selenate. When the T atom sits on a site of tetrahedral crystallographic symmetry, three-dimensional frustrated lattices, such as those belonging to the pyrochlore family, may be produced.^[2] Location of the T atom on a three-fold axis can produce a two-dimensional frustrated lattice, such as the kagomé net.^[6] Many more frustrated topologies are possible in two dimensions. Some, such as the kagomé lattice, may be derived from the triangular lattice by removal of a fraction of the nodes. Others are the result of combining triangles with other shapes, such as squares.^[7] In practice, the T atom may lie somewhere other than a high-symmetry site; this will lead to lattice distortions and deviations from ideal physical behavior. However, some topologies have few real-life examples. In fact, many frustrated topologies have been envisioned, for which predictions of magnetic behavior have been made,^[7] but for which there are no model compounds. One example can be derived from the triangular lattice by removal of 1/7 of the nodes. This approach produces a lattice with connectivity five that has been referred to as the “maple leaf” lattice.^[8] Herein, we

[*] Dr. D. Cave, F. C. Coomer, E. Molinos, Dr. P. T. Wood
University Chemical Laboratory
Lensfield Rd, Cambridge, CB2 1EW (UK)
Fax: (+44) 1223-336-017
E-mail: ptw22@cam.ac.uk

Dr. H.-H. Klauss
Institut für Physik der Kondensierten Materie
Technische Universität Braunschweig (Germany)

[**] We wish to thank Prof. Dieter Fenske (Universität Karlsruhe) for collecting some of the X-ray diffraction data, and Dr. John E. Davies and Dr. Andrew D. Bond (University of Southern Denmark) for help with crystallography in Cambridge. This work was supported by the EPSRC. M = Na, x = 11; M = K, x = 11, M = Rb, x = 10.



Supporting information for this article is available on the WWW under <http://www.angewandte.org> or from the author.

report the synthesis of a family of iron coordination solids which have this topology.

Reaction of anhydrous iron(III) chloride with alkali-metal salts of the ligand *N*-phosphinomethyliminodicarboxylic acid, $\text{H}_2\text{O}_3\text{PCH}_2\text{N}(\text{CH}_2\text{CO}_2\text{H})_2$ (PMIDA) in superheated methanol yields $\text{M}_x[\text{Fe}(\text{O}_2\text{CCH}_2)_2\text{NCH}_2\text{PO}_3]_6 \cdot n\text{H}_2\text{O}$ (**1** $\text{M} = \text{Na}$, $x = 11$; **2** $\text{M} = \text{K}$, $x = 11$; **3** $\text{M} = \text{Rb}$, $x = 10$) as green-yellow octahedra (**1**) and green hexagonal plates (**2** and **3**), respectively. In all cases, the compounds are formed along with colorless crystals of alkali metal halide, which must be removed by sieving. The connectivity of the network in all three compounds is the same, but the average oxidation state of the iron and the space group of the crystals is different. Compound **1** is the most symmetrical, crystallizing^[9] in space group $R\bar{3}$ with one FeL fragment ($\text{L} = (\text{O}_2\text{CCH}_2)_2\text{NCH}_2\text{PO}_3$) in the asymmetric unit (Figure 1).

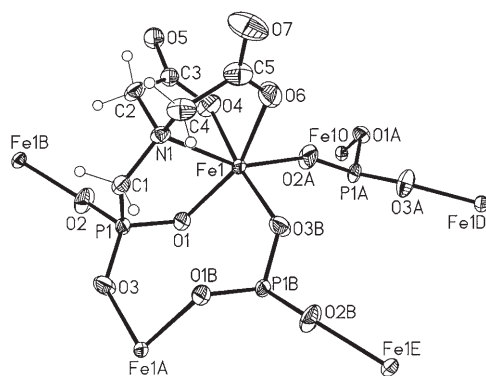


Figure 1. View of the asymmetric unit of **1** with attached symmetry equivalent phosphonate groups and iron ions. Thermal ellipsoids are set at 50 % probability. Selected bond lengths are given in the Supporting Information.

One ligand occupies four coordination sites around the iron atom, and two additional oxygen atoms from the phosphonate groups of other ligands occupy another two sites, completing a distorted octahedral coordination sphere. Hence, the iron atom is bridged to five equivalent metal centers by three phosphonate groups. Four of the iron atoms are linked by simple Fe-O-P-O-Fe bridges, whilst the fifth is linked by two such bridges to form an $(\text{-Fe-O-P-O-})_2$ eight-membered ring. There are also two types of $(\text{-Fe-O-P-O-})_6$ rings formed around three-fold axes in the structure, one of which is centered on the $\bar{3}$ site (Figure 2). These rings link together to generate a two-dimensional lattice, as shown in Figure 3. We can consider the topology of the lattice by joining the iron centers linked by phosphonate bridges. This generates a defect variant of the triangular lattice, in which 1/7 of the nodes are missing (Figure 4). The magnetic ground-state structure of $S = 1/2$ ions on this lattice has recently been considered from a theoretical perspective,^[8] but, to our knowledge, no other real examples of this topology have been described.

The structures of **2** and **3** have the same connectivity, but lower symmetry, crystallizing in space groups $P3_1$ and $C2/c$, respectively.^[9] In both cases, there are six FeL moieties in the

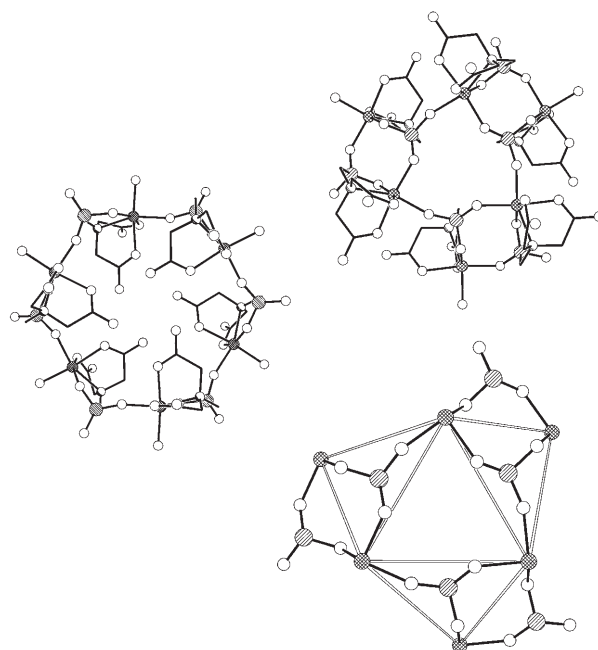


Figure 2. Hexagonal (left) and triangular (right) building blocks in compound **1**; Fe crosshatched circles, P striped circles, O open circles. In the bottom right picture, only the Fe, P, and O atoms are illustrated to emphasize the four fused-triangle motif.

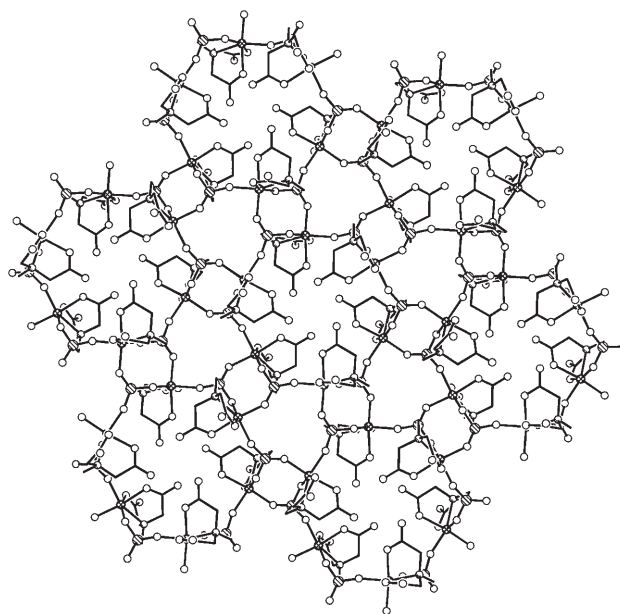


Figure 3. A packing diagram showing part of a layer in compound **1**; Fe crosshatched circles, P striped circles, O open circles.

asymmetric unit, along with many alkali-metal sites. The Fe sites are all fully occupied but some of the K/Rb sites appear to have fractional occupancies. We have investigated the correct stoichiometry of the Rb site in **3** by performing full elemental analysis and by modeling the Fe^{II}/Fe^{III} ratio from the Mössbauer spectrum. These methods give broad agreement for an Rb/Fe ratio of 10:6 and an Fe^{II}/Fe^{III} ratio of 4:2. This result is similar to that obtained by refinement of the

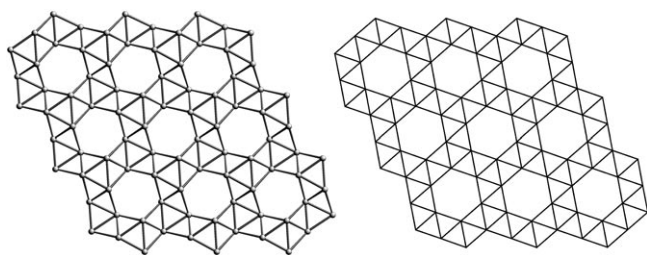


Figure 4. The superexchange lattice in compound **1** (left; Fe circles) and the idealized maple leaf lattice (right).

rubidium-site occupancy in the X-ray structure determination. Refinement of the occupancies of the K sites in **2** gives a K/Fe ratio of 11:6, which requires an Fe^{II}/Fe^{III} ratio of 5:1. For both compounds there is a wide variation in the metal–ligand bond lengths, which is consistent with a variety of average oxidation states for the six crystallographically distinct Fe sites in each structure (see Supporting Information).

The magnetic behavior of **1–3** was investigated using a Quantum Design MPMS5 SQUID magnetometer. Field-cooled magnetization measurements were recorded between 5 and 300 K at 100 G, and isothermal magnetization measurements were recorded between 0 and 5 T at 5 K. There is no indication of long-range order in the temperature-dependent susceptibility measurements (Figure 5), nor is there any sign

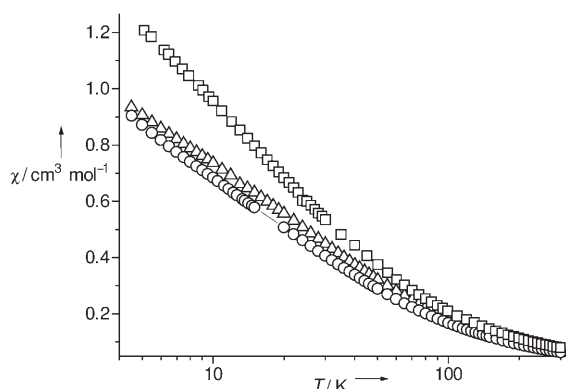


Figure 5. Temperature dependence of the magnetic susceptibility of compounds **1** (□), **2** (○), and **3** (△).

of a broad maximum characteristic of short-range antiferromagnetic order. Plots of χ^{-1} versus T obey the Curie–Weiss law at all temperatures. The Weiss constants Θ are suggestive of moderate antiferromagnetic coupling ($-21(1)$, $-20.5(2)$, and $-17.2(2)$ K for compounds **1**, **2**, and **3**, respectively) and the Curie constants C are consistent with the Fe oxidation-state assignments ($25.3(1)$, $20.21(3)$, and $21.73(3)$ cm³ mol⁻¹ K for compounds **1**, **2**, and **3**, respectively). The Fe–O–P–O–Fe superexchange pathway is clearly quite weak, but the extent of magnetic frustration in these lattices is sufficient to prevent order down to the low-temperature limit of our measurements ($T_N < |\Theta|/4$) and the interlayer separation is sufficient to prevent long-range order mediated by dipolar coupling.

A recent article encourages the development of new strategies for preparing frustrated lattices.^[10] The use of

ligands incorporating triangular templates that are also superexchange pathways, such as the one employed herein, is one approach. However, it is difficult to control the topology of the lattices generated in this way. If we consider the case of the ligand employed herein, nitrogen and carboxylate donors account for three of the six coordination sites around the metal, and the phosphonate oxygen atoms take up the remaining three. Since each phosphonate group can link the central metal atom to two others, each iron center could, in theory, be linked to six neighbors, giving a triangular lattice. In practice, the steric demands of linking the central metal atom to six neighboring FeL moieties is too great. The steric pressure is, therefore, reduced by forming two phosphonate bridges to one adjacent FeL moiety, thereby reducing the connectivity of the lattice to five. This five-fold connectivity could also produce the trellis lattice, which is a much more anisotropic arrangement than the maple leaf lattice, or the T6 lattice, which is a much more compact arrangement (Figure 6). Serendipity is, therefore, involved, not only in the

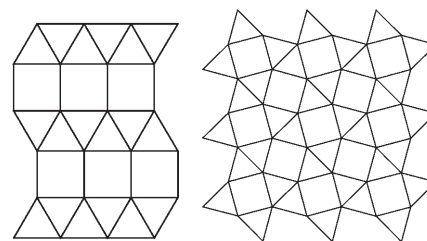


Figure 6. Other lattices with five-fold connectivity: the trellis lattice (left) and the T6 lattice (right).

resultant connectivity, but also in the “choice” of topology. The role of chance is further illustrated by the work of Clearfield and co-workers, who have studied this, and other, phosphonate ligands extensively.^[11] They have found many other interesting coordination modes that compete with the formation of frustrated networks.

Experimental Section

1: Anhydrous FeCl₃ (0.25 g, 1.54 mmol) and NaI (2 g, 13.3 mmol) were added to a stirred solution of H₂O₃PCH₂N(CH₂CO₂H)₂ (0.440 g, 1.94 mmol) and NaOH (0.308 g, 7.7 mmol) in methanol (10 mL). The resulting yellow slurry was placed in a 23-mL teflon-lined autoclave and heated at 200°C for 43 h, and then cooled to room temperature over 5 h. The resulting green-yellow octahedral crystals were removed from the solution by pipette, washed with methanol, sonicated, and sieved through a 63-micron sieve. The resulting crystals were then dried under vacuum. Yield: 94 mg (18 % based on Fe). Elemental analysis calcd (%) for C₃₀Fe₆H₄₈N₆Na₁₁O₄₈P₆: C 17.1, H 2.4, N 4.1, P 9.1; found C 16.9, H 2.3, N 4.0, P 8.9.

2: The reaction between H₂O₃PCH₂N(CH₂CO₂H)₂ (0.440 g, 1.94 mmol), KOH (0.425 g, 7.57 mmol), and anhydrous FeCl₃ (0.25 g, 1.54 mmol) was carried out in the manner described for compound **1**. Compound **2** was isolated in a similar manner to compound **1**, but with the omission of the sieving, as green hexagonal plate-like crystals. Yield: 253 mg (46 % based on Fe). Elemental analysis calcd (%) for C₃₀Fe₆H₄₀K₁₁N₆O₄₄P₆: C 16.8, H 1.9, N 3.9, P 8.7; found C 16.7, H 1.9, N 3.6, P 8.4.

3: $\text{H}_2\text{O}_3\text{PCH}_2\text{N}(\text{CH}_2\text{CO}_2\text{H})_2$ (0.440 g, 1.94 mmol), RbOH (0.776 g, 7.57 mmol), and anhydrous FeCl_3 (0.25 g, 1.54 mmol) were treated in an identical manner to **2** to give green hexagonal plates of compound **3**. Isolated yield: 359 mg (54% based on Fe). Elemental analysis calcd (%) for $\text{C}_{30}\text{Fe}_6\text{H}_{40}\text{N}_6\text{O}_{44}\text{P}_6\text{Rb}_{10}$: C 14.1, H 1.6, N 3.3, Fe 13.1, Rb 33.3; found C 14.0, H 1.7, N 3.0, Fe 14.7(± 0.9), Rb 30.1(± 1.3).

Received: August 10, 2005

Published online: December 21, 2005

Keywords: geometric frustration · hydrothermal synthesis · iron · magnetic properties · phosphonates

their parent atoms. 562 parameters, $R1 = 0.0797$ (for reflections with $I > 2\sigma(I)$), $wR2 = 0.2055$ (all data), $S = 1.035$, largest peak (hole) 1.527(−1.023).

[10] A. Harrison, *J. Phys. Condens. Matter* **2004**, *16*, S553.

[11] See, for example, J. G. Mao, A. Clearfield, *Inorg. Chem.* **2002**, *41*, 2319.

- [1] J. E. Greedan, *J. Mater. Chem.* **2001**, *11*, 37, and references therein.
- [2] S. H. Lee, C. Broholm, C. Ratcliff, G. Gasparovic, Q. Huang, T. H. Kim, S. W. Cheong, *Nature* **2002**, *418*, 856.
- [3] V. Fritsch, J. Hemberger, N. Buttgen, E. W. Scheidt, H. A. K. von Nidda, A. Loidl, V. Tsurkan, *Phys. Rev. Lett.* **2004**, *92*, 116401.
- [4] S. T. Bramwell, M. J. P. Gingras, *Science* **2001**, *294*, 1495.
- [5] J. Snyder, J. S. Slusky, R. J. Cava, P. Schiffer, *Nature* **2001**, *413*, 48.
- [6] A. S. Wills, A. Harrison, C. Ritter, R. I. Smith, *Phys. Rev. B* **2000**, *61*, 6156.
- [7] J. Richter, J. Schulenberg and A. Honecker in *Quantum Magnetism* (Eds.: U. Schollwöck, J. Richter, D. J. J. Farnell, R. F. Bishop), Springer, Berlin, **2004**.
- [8] D. Schmalfuss, P. Tomczak, J. Schulenburg, J. Richter, *Phys. Rev. B* **2002**, *65*, 224405; Z. F. Wang, B. W. Southern, *Phys. Rev. B* **2003**, *68*, 094419.
- [9] Data were collected using a Stoe IPDS diffractometer at the Institut für Anorganische Chemie der Universität Karlsruhe, for compound **1**, and an Enraf-Nonius KappaCCD diffractometer at the University of Cambridge for compounds **2** and **3**. CCDC-279857, CCDC-279858, and CCDC-279859 (compounds **1** to **3**) contain the supplementary crystallographic data for this paper. These data can be obtained free of charge from The Cambridge Crystallographic Data Centre via www.ccdc.cam.ac.uk/data_request/cif. Crystal data for **1**: rhombohedral, $R\bar{3}$, $a = 14.074(2)$, $c = 27.515(6)$ Å, $V = 4719.9(19)$ Å³, $\theta_{\text{max}} = 31.63^\circ$, $\lambda = 0.71073$ Å, $T = 200(2)$ K, 11 821 measured reflections of which 2615 were unique ($R_{\text{int}} = 0.0312$), 2518 reflections had $I > 2\sigma(I)$. The structure was solved by direct methods and refined against F^2 using SHELXTL software. All non-hydrogen atoms were refined anisotropically, and hydrogen atoms were allowed to ride on their parent atoms. 168 parameters, $R1 = 0.0367$ (for reflections with $I > 2\sigma(I)$), $wR2 = 0.0917$ (all data), $S = 1.040$, largest peak (hole) 1.101(−0.848). Crystal data for **2**: trigonal, $P3_1$, $a = 14.3858(3)$, $c = 29.1666(7)$ Å, $V = 5227.4(2)$ Å³, $\theta_{\text{max}} = 25.03^\circ$, $\lambda = 0.71073$ Å, $T = 180(2)$ K, 12 765 measured reflections of which 9489 were unique ($R_{\text{int}} = 0.0307$), 8580 reflections had $I > 2\sigma(I)$. The structure was solved by direct methods and refined against F^2 using SHELXTL software. All non-hydrogen atoms were refined anisotropically, and hydrogen atoms were allowed to ride on their parent atoms. 956 parameters, $R1 = 0.0553$ (for reflections with $I > 2\sigma(I)$), $wR2 = 0.1423$ (all data), $S = 1.068$, largest peak (hole) 1.248(−0.629). Crystal data for **3**: monoclinic, $C2/c$, $a = 24.3559(12)$, $b = 13.6490(5)$, $c = 27.515(6)$ Å, $\beta = 96.722(2)^\circ$, $V = 13 718.7(11)$ Å³, $\theta_{\text{max}} = 22.44^\circ$, $\lambda = 0.71073$ Å, $T = 180(2)$ K, 19 048 measured reflections of which 7290 were unique ($R_{\text{int}} = 0.0678$), 5396 reflections had $I > 2\sigma(I)$. The structure was solved by direct methods and refined against F^2 using SHELXTL software. The Rb, Fe, P, and N atoms were refined anisotropically, the C and O atoms were refined isotropically, and the hydrogen atoms were allowed to ride on